

Elasto Hydrodynamic Lubrication

T. Lubrecht

LaMCoS, INSA-Lyon, France

May 28, 2018

Outline

Outline

- ▶ **Introduction**

Outline

- ▶ **Introduction**
- ▶ Reduced Geometry & Non-Conforming

Outline

- ▶ **Introduction**
- ▶ Reduced Geometry & Non-Conforming
- ▶ EHL Characteristics

Outline

- ▶ **Introduction**
- ▶ Reduced Geometry & Non-Conforming
- ▶ EHL Characteristics
- ▶ **Equations**

Outline

- ▶ **Introduction**
- ▶ Reduced Geometry & Non-Conforming
- ▶ EHL Characteristics
- ▶ **Equations**
- ▶ **Hertzian Solution**

Outline

- ▶ **Introduction**
- ▶ Reduced Geometry & Non-Conforming
- ▶ EHL Characteristics
- ▶ **Equations**
- ▶ **Hertzian Solution**
- ▶ one dimensional

Outline

- ▶ **Introduction**
- ▶ Reduced Geometry & Non-Conforming
- ▶ EHL Characteristics
- ▶ **Equations**
- ▶ **Hertzian Solution**
- ▶ one dimensional
- ▶ two dimensional

Outline

- ▶ **Introduction**
- ▶ Reduced Geometry & Non-Conforming
- ▶ EHL Characteristics
- ▶ **Equations**
- ▶ **Hertzian Solution**
- ▶ one dimensional
- ▶ two dimensional
- ▶ **Lubricated Solution**

Outline

- ▶ **Introduction**
- ▶ Reduced Geometry & Non-Conforming
- ▶ EHL Characteristics
- ▶ **Equations**
- ▶ **Hertzian Solution**
- ▶ one dimensional
- ▶ two dimensional
- ▶ **Lubricated Solution**
- ▶ Ertel Grubin Analysis

Outline

- ▶ **Introduction**
- ▶ Reduced Geometry & Non-Conforming
- ▶ EHL Characteristics
- ▶ **Equations**
- ▶ **Hertzian Solution**
- ▶ one dimensional
- ▶ two dimensional
- ▶ **Lubricated Solution**
- ▶ Ertel Grubin Analysis
- ▶ Dowson Higginson

Outline

- ▶ **Introduction**
- ▶ Reduced Geometry & Non-Conforming
- ▶ EHL Characteristics
- ▶ **Equations**
- ▶ **Hertzian Solution**
- ▶ one dimensional
- ▶ two dimensional
- ▶ **Lubricated Solution**
- ▶ Ertel Grubin Analysis
- ▶ Dowson Higginson
- ▶ Hamrock Dowson

Outline

- ▶ **Introduction**
- ▶ Reduced Geometry & Non-Conforming
- ▶ EHL Characteristics
- ▶ **Equations**
- ▶ **Hertzian Solution**
- ▶ one dimensional
- ▶ two dimensional
- ▶ **Lubricated Solution**
- ▶ Ertel Grubin Analysis
- ▶ Dowson Higginson
- ▶ Hamrock Dowson
- ▶ Moes Venner

Introduction

Three questions for successful operation and optimisation

Introduction

Three questions for successful operation and optimisation

- ▶ Will it work?

Introduction

Three questions for successful operation and optimisation

- ▶ **Will it work?**
 - ▶ *Avoid instantaneous failure.*

Introduction

Three questions for successful operation and optimisation

- ▶ **Will it work?**
 - ▶ *Avoid instantaneous failure.*
- ▶ **How much does it require to work?**

Introduction

Three questions for successful operation and optimisation

- ▶ **Will it work?**
 - ▶ *Avoid instantaneous failure.*
- ▶ **How much does it require to work?**
 - ▶ *Avoid waste of energy/material/money.*

Introduction

Three questions for successful operation and optimisation

- ▶ **Will it work?**
 - ▶ *Avoid instantaneous failure.*
- ▶ **How much does it require to work?**
 - ▶ *Avoid waste of energy/material/money.*
- ▶ **Will it last?**

Three questions for successful operation and optimisation

- ▶ **Will it work?**
 - ▶ *Avoid instantaneous failure.*
- ▶ **How much does it require to work?**
 - ▶ *Avoid waste of energy/material/money.*
- ▶ **Will it last?**
 - ▶ *Avoid premature/dangerous failure.*

Examples

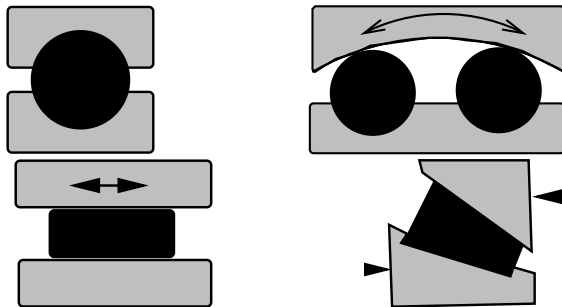


Figure *Sketch of a DGBB, SABB, CRB and TRB cross section.*

Will it Work

compute contact pressure (p_h)

as the contact area is small ($< R$)
the geometry can be approximated
by a parabola

Reduced Geometry

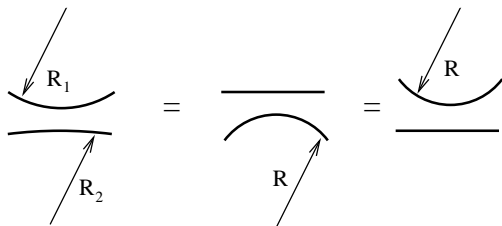


Figure Equivalent geometries $1/R = 1/R_1 + 1/R_2$.

$$H(X) = H_0 + \frac{X^2}{2R} + \dots \quad (\text{parabolic approximation})$$

examples: contact types in a car engine

conforming - non-conforming

Non Conforming Contacts

load w is important

contact area b small with respect to R

pressure p_h very high

ratio deformation to film δ/h very important

compute h , p_h , b and δ

EHL Characteristics

- important piezo-viscous effects

$$\eta(p_h) \gg \eta_0$$

- important elastic effects

$$\delta \gg h_c$$

- contact close to Hertzian conditions

$$p(x, y) \simeq p_h \sqrt{1 - (x/a)^2 - (y/a)^2}, \quad h(x, y) \simeq h_c$$

EHL Trends

- increased load: decreased film, pressure more Hertzian

$$w \nearrow: h \searrow, p \rightarrow p_h$$

- decreased speed: decreased film, pressure more Hertzian

$$u \searrow: h \searrow, p \rightarrow p_h$$

- both effects make the contact more Hertzian
(character of equations becomes more Hertzian)

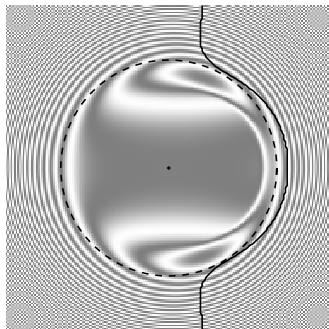
Equations

Reynolds equation:

$$\underbrace{\frac{\partial}{\partial x} \left(\frac{\rho h^3}{12\eta} \frac{\partial p}{\partial x} \right) + \frac{\partial}{\partial y} \left(\frac{\rho h^3}{12\eta} \frac{\partial p}{\partial y} \right)}_{\text{poiseuille}} - \underbrace{\frac{\partial(u_m \rho h)}{\partial x}}_{\text{couette}} - \underbrace{\frac{\partial(\rho h)}{\partial t}}_{\text{transient}} = 0$$

Cavitation

Cavitation Condition: $p \geq 0$.



Elastic Deformation

$$h(x, y) = h_0 + \frac{x^2}{2R_x} + \frac{y^2}{2R_y} + \frac{2}{\pi E'} \int_{-\infty}^{+\infty} \int_{-\infty}^{+\infty} \frac{p(x', y') dx' dy'}{\sqrt{(x - x')^2 + (y - y')^2}}$$

Density Pressure relation

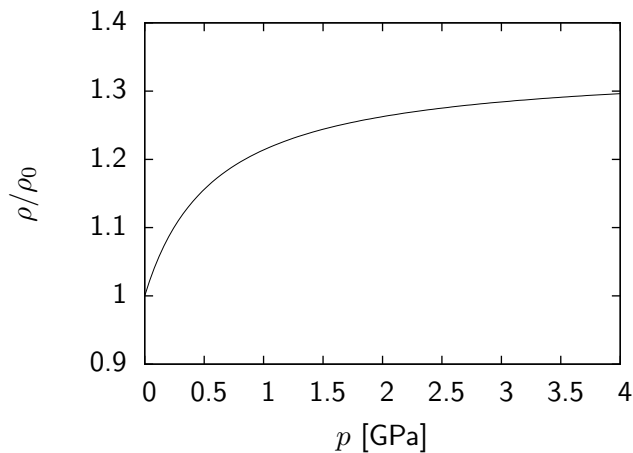


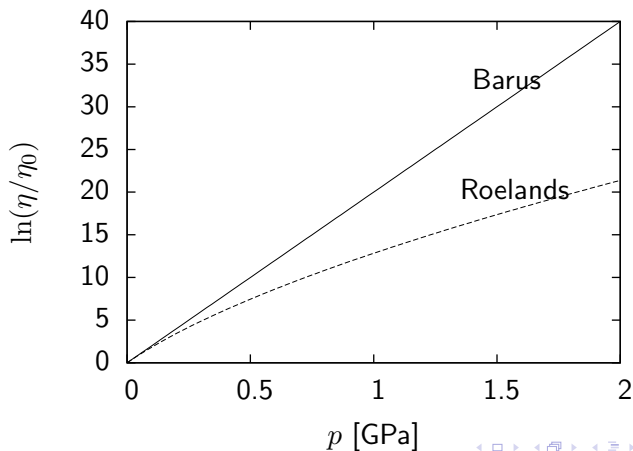
Figure *Relative density ρ/ρ_0 as a function of p .*

$$\rho(p) = \rho_0 \frac{5.9 \cdot 10^8 + 1.34p}{5.9 \cdot 10^8 + p}$$

Viscosity Pressure relation

$$\eta(p) = \eta_0 \exp(\alpha p)$$

$$\eta(p) = \eta_0 \exp \left[\ln(\eta_0) + 9.67 \left\{ -1 + \left(1 + \frac{p}{p_0} \right)^z \right\} \right]$$



Force Balance

$$w = \int_{-\infty}^{+\infty} \int_{-\infty}^{+\infty} p(x', y') dx' dy'$$

Dimensionless Equations

Reynolds Equation with $P = p/p_h$, $X = x/a$, $Y = y/a$ and $H = hR_x/a^2$, based on Hertz and $T = u_m t/a$, $\bar{\eta} = \eta/\eta_0$ and $\bar{\rho} = \rho/\rho_0$.

$$\frac{\partial}{\partial X}(\epsilon \frac{\partial P}{\partial X}) + \frac{\partial}{\partial Y}(\epsilon \frac{\partial P}{\partial Y}) - \frac{\partial(\bar{\rho}H)}{\partial X} - \frac{\partial(\bar{\rho}H)}{\partial T} = 0$$

Where $\epsilon = (\bar{\rho}H^3)/(\bar{\eta}\lambda)$, and $\lambda = (12\eta_0 u_m R_x^2)/(a^3 p_h)$.

Film Thickness equation

$$H(X, Y) = H_0 + \frac{X^2}{2} + \frac{Y^2}{2} + \frac{2}{\pi^2} \int_{-\infty}^{+\infty} \int_{-\infty}^{+\infty} \frac{P(X', Y') dX' dY'}{\sqrt{(X - X')^2 + (Y - Y')^2}}$$

Force Balance equation

$$\int_{-\infty}^{+\infty} \int_{-\infty}^{+\infty} P(X', Y') dX' dY' = \frac{2\pi}{3}$$

Hertzian Solution

The Hertzian solution is the solution of the dry contact problem found by H. Hertz (1881). This approximation neglects the film thickness (h) with respect to the elastic deformation (δ). As a consequence, the solution accurately predicts the maximum (Hertzian) pressure (p_h), contact area (a and b) (and stresses τ) and deformation (δ). Obviously, the film thickness prediction is useless!

The Hertzian prediction becomes more and more accurate whenever the velocity (u) becomes small or the load (w) becomes large ($h \rightarrow 0$).

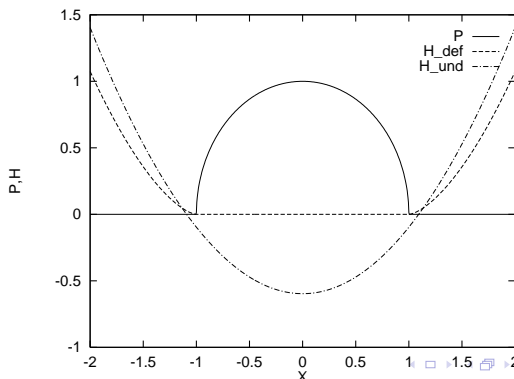
Q: what is the influence of the viscosity η_0 ?

Hertzian Parameters

the line contact Hertzian pressure:

$$\frac{p(x/b)}{p_h} = P(X) = \begin{cases} \sqrt{1 - X^2}, & \text{if } |X| \leq 1; \\ 0, & \text{otherwise.} \end{cases}$$

$$p_h = \frac{2w_1}{\pi b} \quad b = \sqrt{\frac{8w_1 R}{\pi E'}} \quad \delta = \left(\frac{1}{4} + \frac{1}{2} \ln 2\right) \frac{b^2}{R} \approx 0.596... \frac{b^2}{R}$$



Hertzian Parameters

the circular contact Hertzian pressure:

$$\frac{p(x/a, y/a)}{p_h} = P(X, Y) = \begin{cases} \sqrt{1 - X^2 - Y^2}, & \text{if } X^2 + Y^2 \leq 1; \\ 0, & \text{otherwise.} \end{cases}$$

$$p_h = \frac{3w}{2\pi a^2} = \frac{E'}{\pi} \sqrt[3]{\frac{3W_2}{2}} \quad a = \sqrt[3]{\frac{3wR_x}{2E'}} = R_x \sqrt[3]{\frac{3W_2}{2}}$$

$$\delta = \frac{a^2}{R_x} = \sqrt[3]{\frac{9w^2}{4E'^2 R_x}} = R_x \sqrt[3]{\frac{9W_2^2}{4}}$$

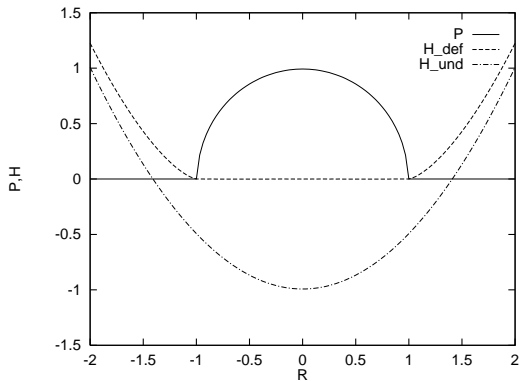


Figure *Dimensionless Hertzian contact pressure, dimensionless deformed and undeformed geometry, for the circular contact case.*

Hertzian Parameters

for the elliptical contact parameters: see course notes.

Ertel Grubin Analysis

The Ertel-Grubin analysis assumes that the lubricated geometry is equal to the Hertzian (dry contact geometry) plus a constant shift. It also assumes that the pressure reaches ∞ at $x = -b$:

($p(x \rightarrow -b) = \infty$). In dimensionless parameters:

($P(X \rightarrow -1) = \infty$). Finally it uses the reduced pressure q .

$$q = \frac{1}{\alpha}(1 - e^{-\alpha p})$$

Thus

$$q(X \rightarrow -1) = \frac{1}{\alpha}$$

Which gives

$$\frac{\partial q}{\partial x} = 6\eta_0(u_1 + u_2) \frac{h - h^*}{h^3}$$

Ertel Grubin Analysis

Integrating between $x = -\infty$ and $x = -b$ using the Hertzian (dry) film thickness $h_h(x)$ gives the Ertel Grubin result.

The EG predictions become more and more accurate for higher loads w and lower speeds u , why?

Ertel Grubin results

$$\frac{h^*}{R} = 1.31 \left(\frac{(\alpha E') \eta_0 (u_1 + u_2)}{E' R} \right)^{3/4} \left(\frac{w_1}{E' R} \right)^{-1/8}$$

Introducing the dimensionless groups: $H^* = h^*/R$,
 $W_1 = w_1/(E'R)$, $U = \eta_0(u_1 + u_2)/(E'R)$, $G = \alpha E'$.
one obtains:

$$H^* = 1.31 (GU)^{3/4} (W_1)^{-1/8}$$

Ertel Grubin graph

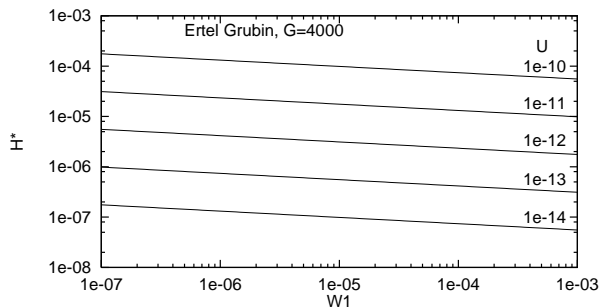


Figure Dimensionless film thickness H^* as a function of W_1 and U for $G=4000$.

Numerical Results

Since the 1960-1970, computers have become sufficiently powerful to solve the complete system of equations: Reynolds equation, film thickness equation and force balance equation. The first solutions were the 1d line contact solutions, whereas in the late 1970's the first point contact solutions were calculated. Using today's computers one can calculate transient EHL solutions of a surface indentation passing through the contact.

Numerical Results, varying U

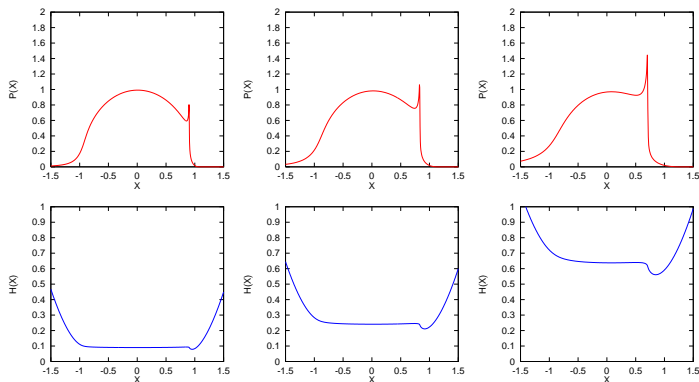


Figure Dimensionless pressure and film thickness distribution
 $W_1 = 1.53 \cdot 10^{-4}$, $U = 5.89, 23.6, 94.2 \cdot 10^{-11}$, $G = 4000$.

Numerical Results, varying U

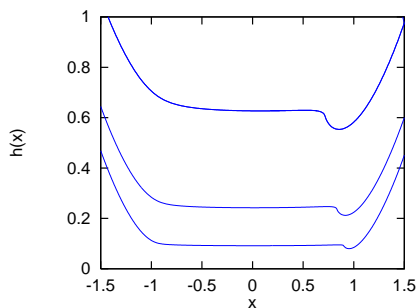
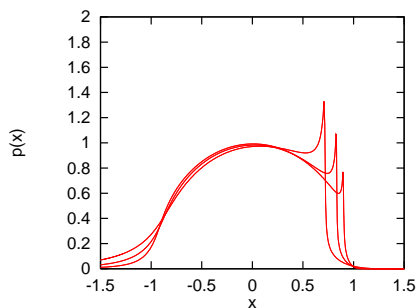


Figure Dimensional pressure and film thickness distribution
 $W_1 = 1.53 \cdot 10^{-4}$, $U = 5.89, 23.6, 94.2 \cdot 10^{-11}$, $G = 4000$.

Numerical Results, varying W_1

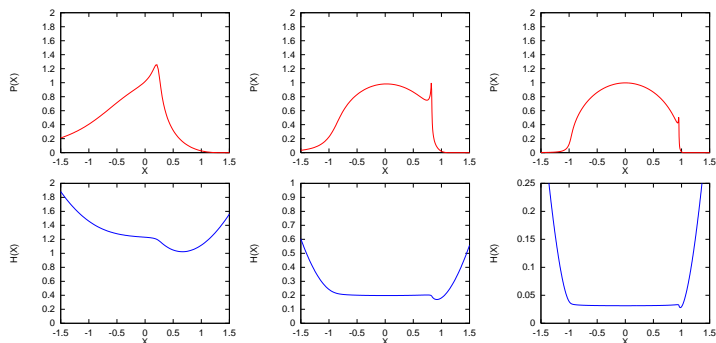


Figure *Dimensionless pressure and film thickness distribution*
 $W_1 = 1.53, 7.67, 38.4 \cdot 10^{-5}$, $U = 5.89 \cdot 10^{-11}$, $G = 4000$.

Numerical Results, varying W_1

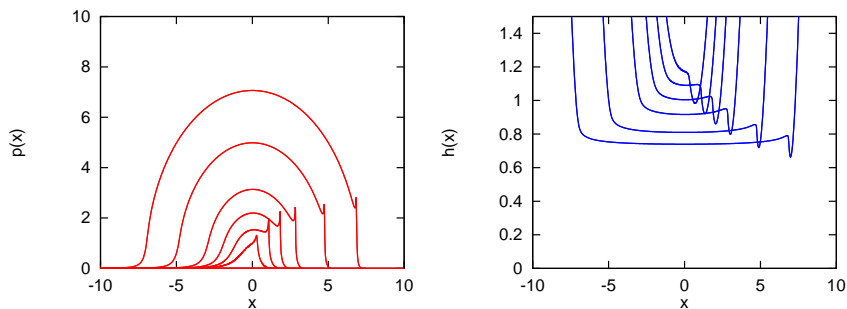


Figure Dimensional pressure and film thickness distribution
 $W_1 = 1.53, 3.84, 7.67, 15.3, 38.4, 76.7 \cdot 10^{-5}$,
 $U = 5.89 \cdot 10^{-11}$, $G = 4000$.

Dowson Higginson 1d

$$H_m = 0.97 G^{0.6} U^{0.7} W_1^{-0.13}$$

where h_m is the minimum film thickness and $H_m = h_m/R$
a comparison of the powers found by Dowson and Higginson with
those of the Ertel Grubin formula

$$H^* = 1.31 (GU)^{3/4} (W_1)^{-1/8}$$

Critical comments

Critical comments

- ▶ The original problem (Reynolds+geometry+force balance) is a two parameter problem: α and λ .

Critical comments

- ▶ The original problem (Reynolds+geometry+force balance) is a two parameter problem: α and λ .
- ▶ The DH solution is a three parameter solution: W , U and G . Furthermore, the DH parameters are NOT $O(1)$!

Critical comments

- ▶ The original problem (Reynolds+geometry+force balance) is a two parameter problem: α and λ .
- ▶ The DH solution is a three parameter solution: W , U and G . Furthermore, the DH parameters are NOT $O(1)$!
- ▶ The more recent Moes-Venner solution is a two parameter solution: M , and L . Furthermore, the Moes parameters M , L and H ARE $O(1)$!

Moes Venner 1d

$$H_{min} = 1.56 L^{0.55} M_1^{-0.125}$$

$$H_{min} = h_m / (R\sqrt{U})$$

$$M_1 = W_1 / \sqrt{U}$$

$$L = G\sqrt[4]{U}$$

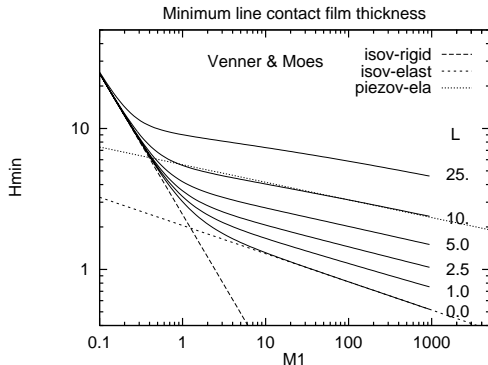


Figure Moes-Venner 1d film thickness prediction.

Comparison of powers

	E.G.	D.H.	M.V.
G	0.75	0.60	0.55
U	0.75	0.70	0.7
W_1	-0.125	-0.13	-0.125

Table Comparison of the powers obtained in the Ertel Grubin, Dowson Higginson and Moes Venner film thickness equations.

Hamrock Dowson 2d

$$H_c = 1.69 G^{0.53} U^{0.67} W_2^{-0.067} (1 - 0.61 \exp(-0.73k))$$

$$H_m = 2.27 G^{0.49} U^{0.68} W_2^{-0.073} (1 - \exp(-0.68k))$$

with $H_c = h_c/R_x$, $W_2 = w/(E' R_x^2)$, $U = \eta_0(u_1 + u_2)/(E' R_x)$,
 $G = \alpha E$.

Moes Venner 2d

using $H_{cen} = h_c / (R_x \sqrt{U})$, $M_2 = W_2 / U^{3/4}$, $L = G \sqrt{U}$.

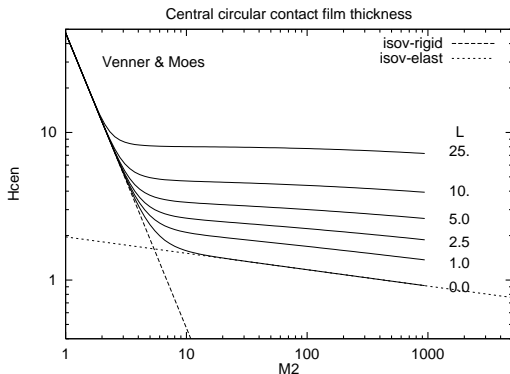


Figure *Moes-Venner 2d film thickness prediction.*

Moes Venner 1d - equations

iso-viscous rigid: $H_m = 2.45M_1^{-1}$

iso-viscous elastic: $H_m = 2.05M_1^{-1/5}$

piezo-viscous elastic: $H_m = 1.56M_1^{-1/8}L^{0.55}$

Moes Venner 2d - equations

iso-viscous rigid: $H_c = 47.3M_2^{-2}$

iso-elastic: $H_c = 1.96M_2^{-1/9}$

Boundary layer analysis

The inlet zone can be considered as a boundary layer between a low pressure (Poiseuille) zone and a high pressure (Couette) zone. Let us study the pressure distribution in the inlet

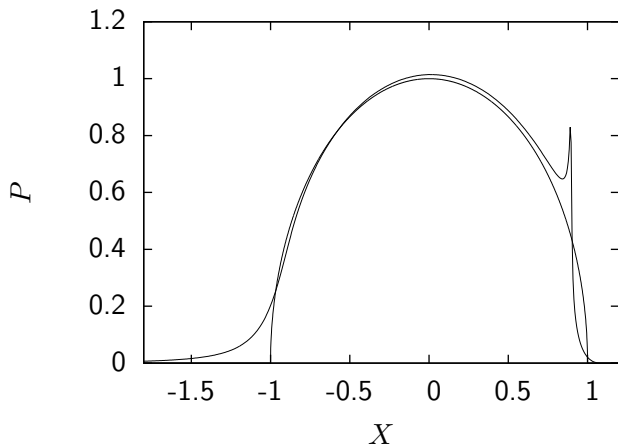


Figure Dimensionless pressure distribution $M = 100$, $L = 10$.

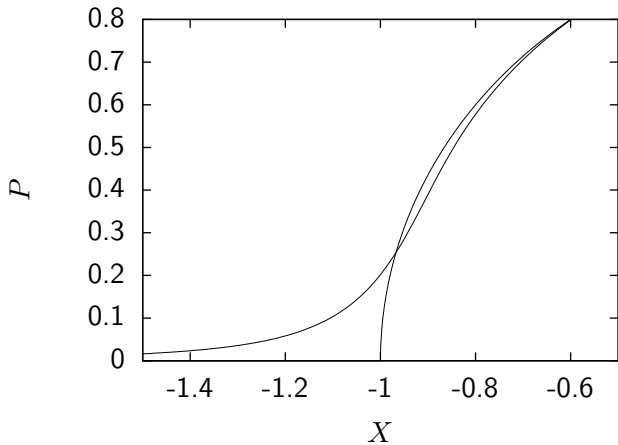


Figure *Zoom around the inlet $X = -1$.*

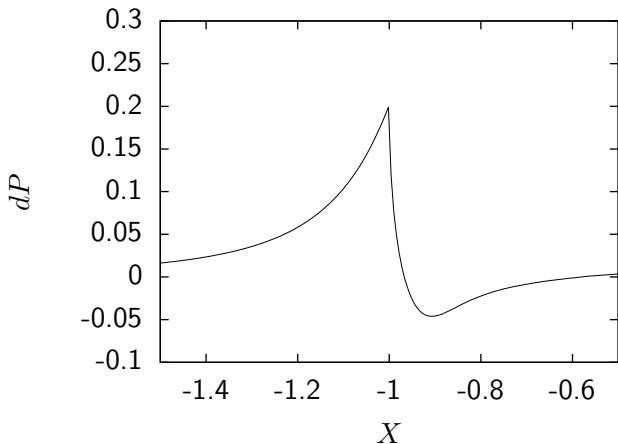


Figure *Dimensionless pressure difference distribution $M = 100$, $L = 10$, around $X = -1$.*

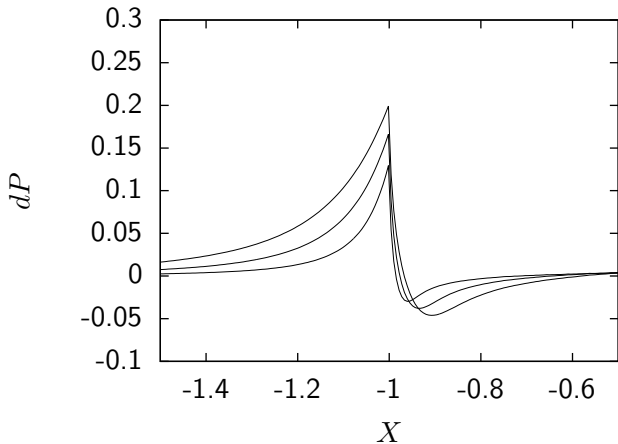


Figure *Dimensionless pressure difference distribution*
 $M = 100, 200, 500, L = 10, \text{ around } X = -1.$

It is clear that coordinate transformations in X and in P are necessary to be able to collapse the inlet pressure distribution onto a single curve:

$$\overline{dP} = dP \sqrt[3]{M} \quad (1)$$

$$\overline{X} = -1 + (X + 1) \sqrt[2]{M} \quad (2)$$

for completeness

$$\overline{H} = H \sqrt[16]{M} \quad (3)$$

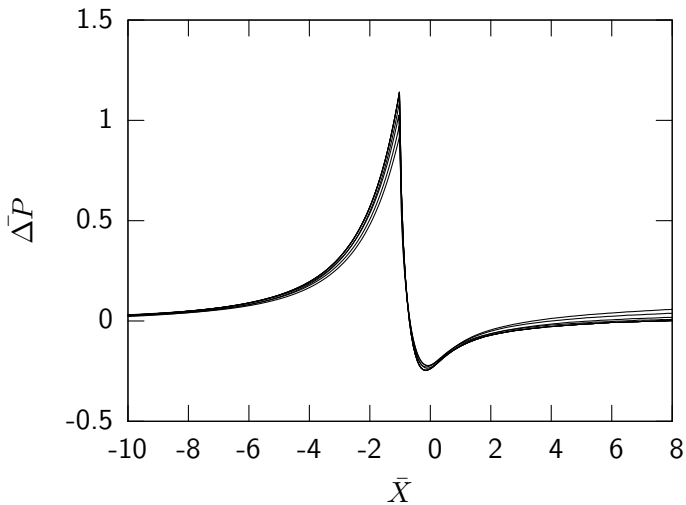


Figure $\bar{\Delta P}$ as a function of \bar{X} for $M = 100, 200, 500 \dots 20000$,
 $L = 10$.